



Research Article

The *irp2* Genes in High Pathogenicity Islands are Involved in the ROS Generation and Increases Antioxidase Levels in the PMNs Caused by Porcine Pathogenic *Escherichia coli*

Yulin Yan*, Xiangfeng Li, Zhaohui Wei, Guowen Fu, Hong Gao*, Ru Zhao, Zhi yong Shao, Weijie Qu and Yongke Sun

Abstract

Polymorphonuclear leukocytes (PMNs) release large quantities of reactive oxygen species (ROS) to kill pathogens. *Escherichia coli* (*E. coli*) strains containing a Yersinia high-pathogenicity island (HPI) display increased virulence that is attributable to increased iron scavenging activity, which enhances bacterial growth and limits the availability of iron for use by innate immune cells. ROS generation requires the catalysis of iron. The *irp2* gene has been confirmed to be the main gene involved in the synthesis of HPI. In the present study, the effect of pathogenic HPI-positive Yunnan-dominant (O_{152}) *E. coli* strains on the respiratory oxidative stress response from PMNs in Yunnan Saba pigs were not explored. The results showed that *E. coli* containing the HPI can reduce ROS generation by competitively consuming iron in the surrounding environment, while inducing high levels of antioxidantases in PMNs. We discovered a novel mechanism by which the HPI protects *E. coli* from ROS and enhances its virulence in PMNs. These results increase our understanding of the interaction between pathogenic *E. coli* and host PMNs in Saba pigs.

Keywords

Porcine pathogenic; *Escherichia coli*; *irp2*; PMNs; Respiratory burst

Introduction

Polymorphonuclear leukocytes (PMNs) are key components of the innate immune system and the first responders to infection or cell injury [1]. These cells play a key role in the host defense against invading pathogens and in inflammatory processes [2]. Within the first minutes of stimulation, PMNs release large quantities of highly toxic reactive oxygen species (ROS) during the so-called "respiratory burst" [3]. The production of ROS is a well-known and efficient microbicidal mechanism. In the presence of increased oxygen free radicals, the cell membrane permeability is disrupted, which is followed by the damage of cells and organelles [4]. Thus, PMNs play a unique role in the immune system as the first line of defense against infection [5].

*Corresponding author: Yulin Yan, Hong Gao, College of Veterinary Medicine, Yunnan Agricultural University, Kunming, PR china, E-mail: yanyulin333@163.com, gaohongping@163.com

Received: July 16, 2018 Accepted: August 04, 2018 Published: August 10, 2018

The respiratory burst of PMNs is characterized primarily by the production of superoxide anion radicals (O_2^-) following a series of stimulating responses [6]. O_2^- is produced by the catalytic action of nicotinamide adenine dinucleotide phosphate (NADPH); however, O_2^- cannot cross the cell membrane [7]. The NADPH oxidase of the phagocyte, a multi-protein complex, exists in the dissociated state in resting cells, converts into the functional oxidase complex upon stimulation, and then generates O_2^- [8]. NADPH can also maintain the reduced state of glutathione (GSH). The antioxidant superoxide dismutase (SOD) can catalyze the O_2^- radical into hydrogen peroxide (H_2O_2). However, H_2O_2 has a low oxidative capacity and cannot kill the bacteria [9]. SOD plays an important role in balancing the oxidant and antioxidant effects [10]. SOD can protect cells from damage by removing ROS. Another antioxidant, glutathione peroxidase (GSH-Px), can also catalyze H_2O_2 to H_2O . GSH-Px is an important, widely expressed enzyme that protects the integrity of membrane structure and function [11].

The O_2^- radical and H_2O_2 together generates the highly active hydroxyl radical ($\cdot HO$) via the Fenton type Haber-Weiss reaction [12,13]. The HO can cause protein peroxidation, deoxyribonucleic acid (DNA) damage, and lipid peroxidation. The final products of lipid peroxidation are methane dicarboxylic aldehyde, which exhibits potent cytotoxicity [14]. The antioxidant effects mostly happen to non-phagocytes [9]. In PMNs, the majority of H_2O_2 is catalyzed into hypochlorous acid (HOCl) by the myeloperoxidase (MPO) in azurophilic granules. HOCl and HO are the major efficient bactericidal products catalyzed from O_2^- and H_2O_2 , respectively [15-17].

Escherichia coli (*E. coli*) contains Yersinia high-pathogenicity island (HPI), which encodes the potent virulent siderophore yersiniabactin [18]. The core functional domain of HPI is the *irp2* gene, which mediates its iron-scavenging activity [19]. The increased virulence of bacteria containing an HPI may be explained by this increased iron-scavenging ability, which would enhance bacterial growth. Increased iron scavenging also limits iron availability to those cells of the innate immune system that require iron to catalyze the Haber-Weiss reaction, which produces $\cdot HO$ [1,20].

Saba pigs are the excellent local breed pigs in the Yunnan province in southwest China. In the present study, the effects of respiratory oxidative stress induced by dominant pathogenic *E. coli* containing an HPI from Yunnan strains (O_{152}) was explored for PMNs from Yunnan Saba pigs. Cell counting was used to detect the population of PMNs. Chemiluminescence was used to detect the levels of total SOD (T-SOD), GSH-Px, and MPO at 4, 8, 12, 16, 20, and 24 h after PMN infection with *E. coli*. An enzyme-linked immunosorbent assay (ELISA) was used to determine the content of NADPH and ROS at different time points. An iron saturation assay was used to investigate whether the HPI-positive *E. coli* reduced the production of ROS via iron uptake.

Methods

Bacterial culture

E. coli of the O_{152} serotype was clinically isolated from the fecal

samples of Yunnan Saba pigs. The isolated strains of *E. coli* O₁₅₂ were stored of 50% glycerol stocks at -80°C. The strains were cultured on Luria-Bertani agar plates overnight at 37°C. Then, a single colony was picked and plated onto Luria-Bertani liquid medium at 37°C. The bacterial concentration was determined based on the optical density at 600 nm, which was between 0.6 and 0.8 colony-forming units (CFU). *E. coli* strains were then serially diluted and plated to enumerate CFU.

Construction of the HPI knockout strain

The construction of the HPI (*irp2* gene) knockout strain was carried out using the Red recombinase system. Target segments were prepared with pKD3 using PCR. The primers P1 and P2 (Table 1) contain FRT and chloramphenicol resistance genes with the *irp2* homologous recombination arm in the 5' region of the forward and reverse primers. Competent cells were prepared by using *E. coli* O₁₅₂. PCR products were purified using a gel extraction kit (BioTeke, Beijing). Purified PCR products were transformed into *E. coli* O₁₅₂-competent cells containing pKD46. LB media containing chloramphenicol were used to screen positive strains at 30°C overnight. The pKD3 primers P3 and P4 (Table 1) was used to identify the positive colony, designated as HPI/ΔHPI/pKD46, which was cultured at 37°C for 16 hours to remove the plasmid pKD46. Primers P5 and P6 (Table 1) were used to confirm the removal of pKD46. The positive colony was designated as HPI/ΔHPI/Cl⁺. The plasmid pCP20 was transformed into HPI/ΔHPI/Cl⁺ competent cells to remove the chloramphenicol resistance gene. Primers P3 and P4 (Table 1) were used to identify the positive colonies, which were designated as ΔHPI. The identification of the knockout strain (ΔHPI) was performed using PCR for the *irp2* gene (Table 1) and western blotting for the HMWP protein (HMWP1, 240 kDa; HMWP2, 228 kDa).

Cell culture and infection of PMNs with *E. coli*

The PMNs were isolated using a kit (TBD, Tianjin, China). The PMNs were added to a 6-well plate in Roswell Park Memorial Institute medium 1640 (RPMI 1640) with 10% fetal bovine serum (HyClone, USA) and antibiotics cultured in a 5% carbon dioxide incubator at 37°C.

HPI-positive *E. coli* was identified using polymerase chain reaction (PCR). The bacteria with and without HPI (ΔHPI) (multiplicity of infection (MOI)=200) were added to the PMNs. The bacteria were washed twice with phosphate-buffered saline (PBS) and resuspended in RPMI 1640. The PMNs were incubated at 37°C for 5 min before the addition of an equal volume of bacterial solution. The assay was further divided into three groups: the control group of the PMNs was exposed to an equal volume of antibiotic-free DMEM, the HPI-infected group, and the ΔHPI-infected group. The PMNs were

cultured at 37°C in 5% carbon dioxide. The samples were collected at 4, 8, 12, 16, 20, and 24 h for subsequent experiments. Each of the experimental groups is with three replicates.

Elisa

The levels of NADPH and ROS were detected using an ELISA Kit (Nanjing Jiancheng Bioengineering Institute, Nanjing, China) according to the manufacturer's instructions.

Iron saturation assay: An iron saturation assay was used to investigate whether the HPI-positive *E. coli* could reduce the production of ROS through iron uptake. The PMNs were infected with *E. coli* with and without HPI. PMNs were treated with varying concentrations of deferoxamine (0, 5, 10, 20, 35, and 80 μm) (Novartis, Switzerland) and PBS (equivalent volume) for 4 h, and the ROS production was quantified.

Chemiluminescence assay: To assess the oxidative burst of PMNs induced by *E. coli*, chemiluminescence was used to detect the levels of T-SOD, GSH-Px, and MPO. The cell suspension and the cells were collected, and the T-SOD, GSH-Px, and MPO levels were detected using the xanthine oxidase assay, GSH-glutathione disulfide assay, and o-dianisidine method (Nanjing Jiancheng Bioengineering Institute, Nanjing, China), respectively.

Statistical analysis: Analysis of variance and multiple comparison analyses were performed using SPSS software, Version 16.0. For duplicate determinations, the error bars to reflect one half of the range; otherwise, they reflect the standard error of the mean. A *P* value of <0.05 was considered statistically significant.

Results

Identification of the knockout strain (ΔHPI)

Identification of the knockout strain (ΔHPI) was performed by PCR detection of the *irp2* gene (357 bp) and western blotting for the HMWP protein (HMWP1, 240 kDa; HMWP2, 228 kDa) (Figure 1). The screening for the *irp2* gene in the knockout strain (sample 2) was negative (Figure 1A), which demonstrated that *irp2* was successfully deleted. In addition, the western blot identification of the HMWP protein in the knockout strain (sample 3) (Figure 1B) was also negative. The above results demonstrated that the knockout strain (ΔHPI) was created successfully.

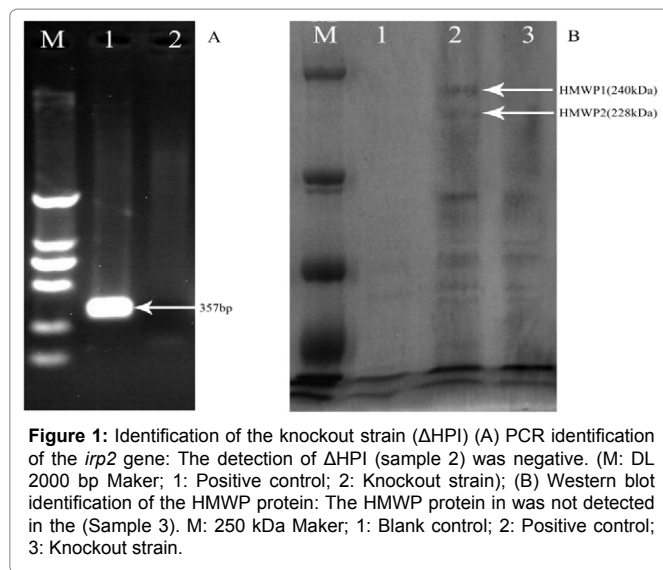
Isolation of the PMNs

The purity of the isolated PMNs by Wright Giemsa staining is shown in Figure 2A. The feature of the PMNs is karyoblobism could be clearly observed. The PMNs were 95% pure. And the viability of the cells stained by Trypan blue is shown in Figure 2B. A colorless and transparent visible living cells are not stained with and a small

Table 1: Primers and sequences.

Primers	Sequence (5'-3')	Product (bp)
P1	gtacattctgtcttaagtcttgagacctctgtctgcccaaggtgtactagACGCATTGTGTAGGCTGGAG	1162
P2	ttaggggatagactgttttagattataacatgatcttgattaaccttggtacTTAACGGCTGCACATGGGAATTAG	
P3	TACATTCTGTCTTAATGTC	1205
P4	GACTGTTTAGATTATTAACA	
P5	TAGCGGATCCTACCTGAC	596
P6	ATCAGTTCCTGTGGGTCG	
<i>irp2</i>	F: CGCTGGTTAGCATTCTGG	357
	R: AATCTGTCCGGCGTTGAG	

Underlined sequences: *irp2* gene homologous recombination



amount of Trypan blue stained by dead cells. The isolated PMNs were 96% viable.

The cytopathic effect on PMNs at different time points

The bacterial colonies used to infect PMNs had the same number of CFUs. PMNs release ROS to kill pathogens. However, if PMNs fail to produce an effective level of ROS, they will be killed by the pathogens. The population of PMNs in the HPI-infected group was dramatically reduced compared to that in the control group and the Δ HPI-infected group. Moreover, in the Δ HPI-infected group, the number of PMNs also decreased, but it was higher than that in the HPI-infected group (Figure 3).

HPI-positive *E. coli* inhibited ROS production

The effects of HPI on the ROS production of PMNs are shown in Figure 4A. Overall, ROS production in the Δ HPI-infected group was higher than that in the HPI-infected group ($P < 0.05$). ROS production in the HPI-infected group was significantly higher than that in the control group ($P < 0.05$) at 4, 8, and 12 h, but it was reduced at the latter three time points. In the Δ HPI-infected group, the ROS production was higher than in the control group ($P < 0.05$). These results indicated that HPI inhibited the ROS response from the PMNs.

To investigate whether the HPI-positive *E. coli* could reduce the production of ROS by taking up iron, an iron saturation assay was performed. HPI-positive *E. coli* encodes yersiniabactin, which provide the bacteria with iron during infection. Moreover, HPI also reduces the iron supply of the innate immune cells. The ROS production in the PBS group was unchanged and higher than that in the deferoxamine group (Figure 4B). ROS generation in the deferoxamine group was decreased gradually as the drug concentration was increased.

These results suggest that the bacteria containing the HPI reduce ROS production in PMNs.

The effect on the activation of NADPH oxidase

NADPH is a key enzyme involved in O_2^- production via the catalysis of O_2 ; this process is called a “respiratory burst”. The HPI-infected group was significantly different from the control group and from the Δ HPI-infected group ($P < 0.05$), except at the 4 h time point (Figure 5). The level of NADPH production in the Δ HPI-infected

group was higher than that in the HPI-infected group ($P < 0.05$) after 8 h. These results showed that PMNs produced more NADPH to kill the Δ HPI bacterium. However, in the HPI-infected group, the production of NADPH was less lower, which indicated that HPI can influence NADPH production.

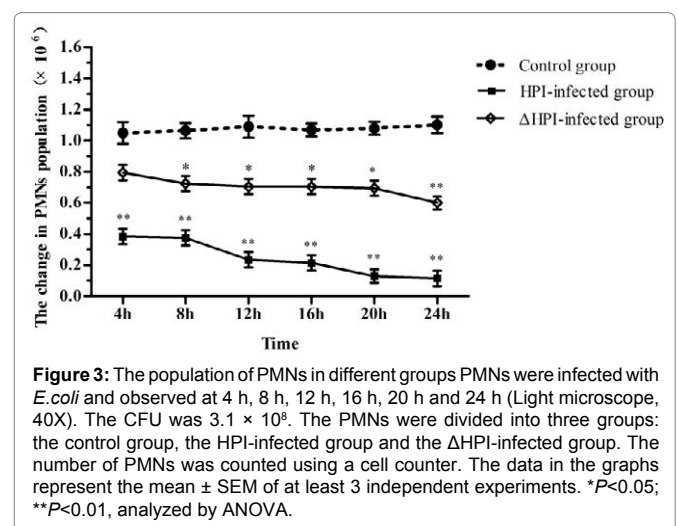
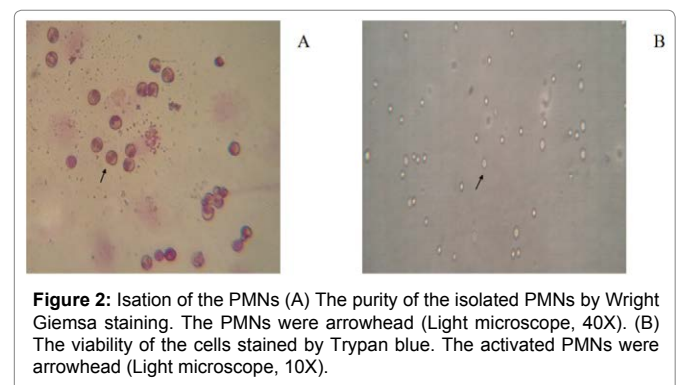
HPI-positive *E. coli* reduced antioxidant enzyme production

T-SOD and GSH-Px are antioxidant enzymes expressed in PMNs. These enzymes can protect PMNs from ROS-mediated damage. T-SOD can catalyze the conversion of O_2^- into H_2O_2 , and H_2O_2 can be catalyzed into H_2O by GSH-Px.

Overall, the T-SOD production in the HPI-infected group was higher than that in the control group and in the Δ HPI-infected group ($P < 0.05$) (Figure 6A). T-SOD production was lower in the Δ HPI-infected group than in the control group ($P < 0.05$) and also showed a trend to decrease further. The production of GSH-Px in the HPI-infected group was higher than that in the control group at 4, 8, and 12 h, but was lower at the latter three time points (Figure 6B) ($P < 0.05$). GSH-Px production was lower in the Δ HPI-infected than in the control group ($P < 0.05$).

The lower production of MPO in HPI-infected group

MPO is a peroxidase expressed in the azurophilic granules of PMNs. The MPO- Fe^{3+} complex can catalyze the conversion of H_2O_2 into HOCl, which can kill pathogens. The MPO levels can also reflect the activity of PMNs [16]. As shown in Figure 7, the production of



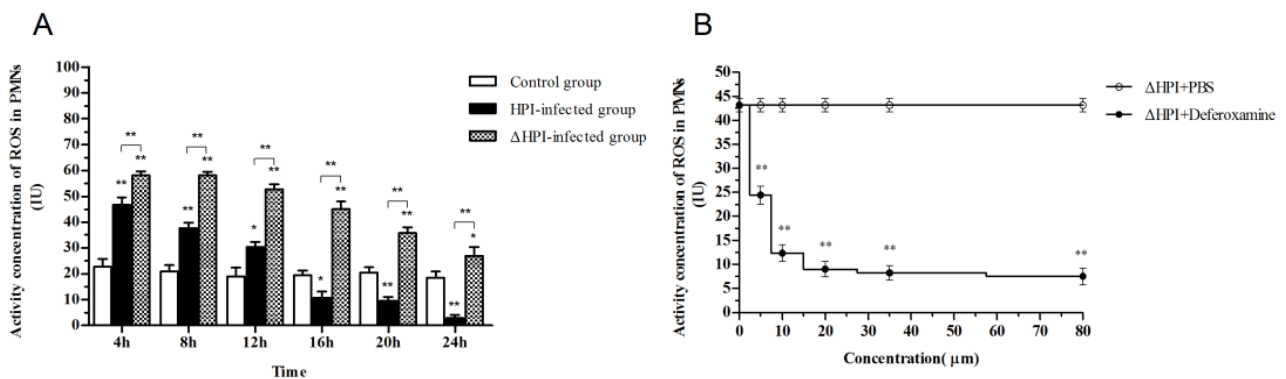


Figure 4: The activity concentration of ROS (IU) in PMNs was detected by ELISA (a) The ROS generation in PMNs at different time point. The PMNs was infected with *E.coli* and detected at 4 h, 8 h, 12 h, 16 h, 20 h and 24 h. The CFU was 3.1×10^8 . The PMNs were divided into three groups: control group, HPI-infected group and Δ HPI-infected group. Data in the graphs represent mean \pm SEM of at least 3 independent experiments. * $P < 0.05$; ** $P < 0.01$, analyzed by ANOVA; (b) The activity concentration of ROS in PMNs (IU). Hollow circle: Δ HPI-infected group was disposed with PBS; Solid circle: Δ HPI-infected group was disposed with deferoxamine.

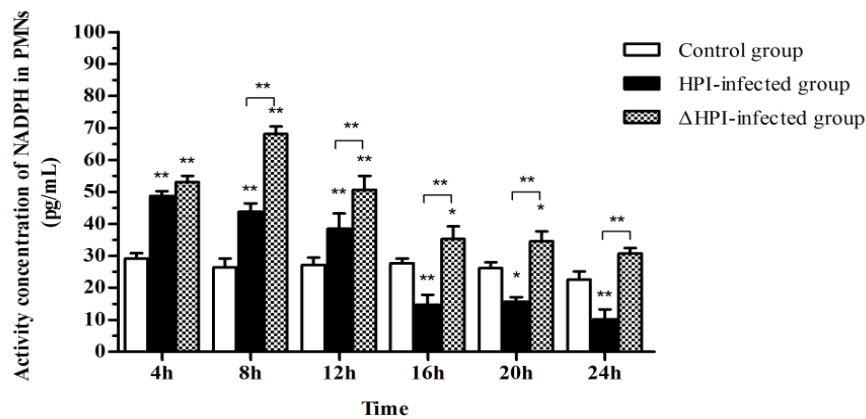


Figure 5: The effect of the high-pathogenicity island (HPI) on activity concentration of nicotinamide adenine dinucleotide phosphate (NADPH) in polymorphonuclear leukocytes (PMNs) (pg/ml). The PMNs were infected with *E.coli* and NADPH was detected at 4, 8, 12, 16, 20, and 24 h. The CFU was 3.1×10^8 . An enzyme-linked immunosorbent assay was performed to detect the concentration of NADPH. The PMNs were divided into three groups: the control group, the HPI-infected group, and the Δ HPI-infected group. The data in the graphs represent the mean \pm SEM of at least 3 independent experiments. * $P < 0.05$; ** $P < 0.01$, analyzed by ANOVA.

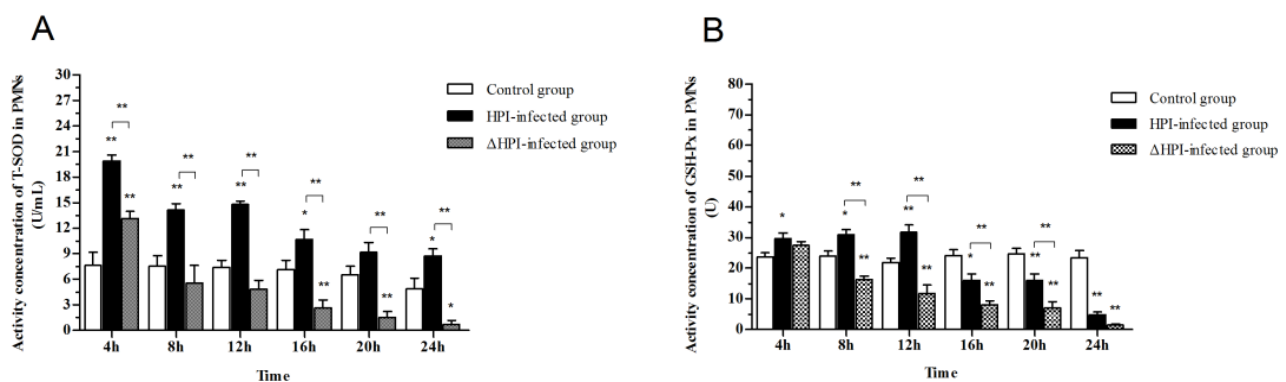


Figure 6: The effect of the high-pathogenicity island (HPI) on the expression of antioxidant enzymes in respiratory burst. The polymorphonuclear leukocytes (PMNs) were infected with *E.coli* and detected at 4, 8, 12, 16, 20, and 24 h post infection. The CFU was 3.1×10^8 . The chemiluminescence method was used to quantify the levels of total superoxide dismutase (T-SOD) and glutathione peroxidase (GSP-Px). The PMNs were divided into three groups: the control group, the HPI-infected group, and the Δ HPI-infected group. The data in the graphs represent the mean \pm SEM of at least 3 independent experiments. * $P < 0.05$; ** $P < 0.01$, analyzed by ANOVA.

(A) Activity concentration of T-SOD (U/mL) in PMNs (B) Activity concentration of GSP-Px (U) in PMNs.

MPO in the HPI-infected group was lower than that in the control group ($P < 0.05$), with a trend toward a further reduction at the latter time points. However, the MPO production in the Δ HPI-infected group was higher than that in the control group and in the HPI-infected group ($P < 0.05$).

Discussion

The population of PMNs in the Δ HPI-infected group was reduced in comparison to the control group; however, it was higher than that in the HPI-infected group. The decreased population of PMNs in the HPI- and Δ HPI-infected groups may have resulted from the bactericidal activity. The intracellular ROS may also activate the genes responsible for apoptosis. ROS can cause DNA damage, which initiates a sequence of events that cause cell suicide [21]. ROS can also induce necrosis by acting as second messengers in the death receptor signaling pathways involved in programmed necrosis [22-23]. In the present study, the sharp decrease of PMNs in the HPI-infected group may have resulted from H_2O_2 interference with ROS signal transduction [24]. H_2O_2 catalysis *via* the Fenton Haber-Weiss reaction was prevented, which resulted in the accumulation of H_2O_2 . This effect increased cytotoxicity and induced the apoptosis and necrosis of PMNs [1,25]. The production of a large number of *E. coli* can lead to excessive nutrient consumption, which can further induce the necrosis of PMNs through starvation. The ability of PMNs to kill pathogens and survive depends on their ability to mount an effective respiratory burst response. The effective production of ROS can ensure PMN survival [26]. ROS production by innate immune cells is inhibited by yersiniabactin, which is produced only by the high-pathogenicity bacteria. Yersiniabactin provides iron to the bacteria and, more importantly, prevents ROS production by innate immune cells [27]. HPI-positive *E. coli* may also increase their pathogenicity by this mechanism.

Iron has been suggested to playing an important role in the production of ROS. A study by Kordower et al. [28] has showed that deferoxamine mesylate exhibits neuroprotective effects on dopaminergic neurons of the nigrostriatal system by reducing oxidative stress [28]. Our results demonstrate that HPI reduces ROS generation by taking up iron. HPI-positive *E. coli* encodes a high-affinity iron acquisition protein, yersiniabactin, that can competitively utilize iron to prevent the ROS and HOCl responses

from the host and escape from being killed [18]. NADPH is a key enzyme in the catalysis of O_2 to produce O_2^- , a process called "respiratory burst." Later, O_2^- leads to the formation of other toxic O_2 metabolites, which also promote microbicidal mechanisms [29]. O_2^- can also be converted to $\cdot OH$ *via* the Fenton Haber-Weiss reaction; $\cdot OH$ has a high cytopathicity and potential to kill pathogens. The results of NADPH generation may indicate that PMNs require more NADPH to generate ROS to kill Δ HPI bacterium [29]. However, in the present study, the production of NADPH was lower in the HPI-infected group (Figure 5). Interestingly, the increased metabolism of H_2O_2 can promote NADPH production [30]. HPI-positive *E. coli* can competitively utilize the iron of PMNs, which can increase H_2O_2 accumulation and reduce bactericidal ROS generation. These results demonstrate that expression of HPI might also influence NADPH production.

Cells have developed a system for maintaining the oxidant-antioxidant balance to protect themselves from damage [10]. The first line of antioxidant defense is SOD, which balances the level of intracellular reactive ROS [31]. SOD can catalyze O_2^- into H_2O_2 , which can be catalyzed into H_2O by GSH-Px. However, this reaction occurs most often in non-phagocytic cells. In PMNs, most H_2O_2 is catalyzed into HOCl and $HO\cdot$ [9,32]. The increased antioxidant levels may be due to reduced antioxidant consumption resulting from decreased ROS generation. In the Δ HPI-infected group, the accumulation of ROS consumed more T-SOD and GSH-Px to create a balance. The H_2O_2 -MPO-HOCl pathway may be important for cytopathogenesis [33]. Low levels of MPO were associated with a low level of HOCl and impaired ability to kill pathogens. Neuroblast phagocytes cannot kill *Staphylococcus aureus* unless the bacteria are coated with MPO. This finding suggested that the respiratory burst was not sufficient to kill the organisms, but the presence of MPO was required [3]. MPO must combine with Fe^{3+} to catalyze H_2O_2 metabolism. HPI-positive *E. coli* can take up iron, which decreases the efficiency of H_2O_2 -MPO-HOCl metabolism. HPI-positive *E. coli* can reduce the bactericidal ability through H_2O_2 -MPO-HOCl pathway by consuming iron [34]. Thus the integral MPO system played an important role in killing bacteria.

Conclusions

The present results demonstrate the intimate relationship between HPI expression and *E. coli* pathogenicity.

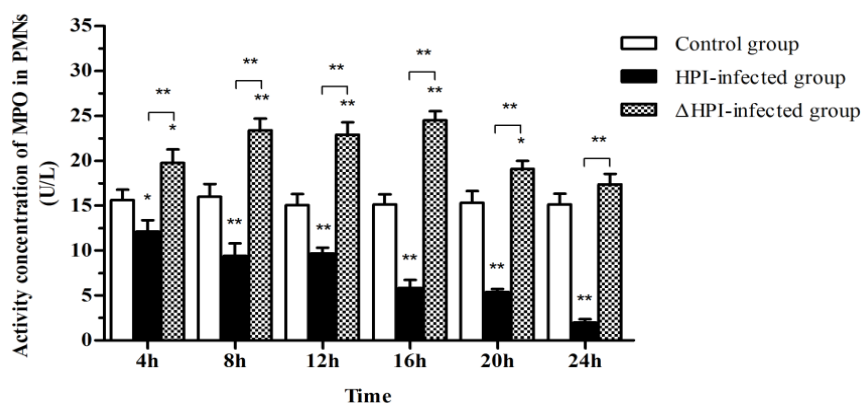


Figure 7: The effect of the high-pathogenicity island (HPI) on the activity concentration of myeloperoxidase (MPO) in polymorphonuclear leukocytes (PMNs) (U/L). The PMNs were infected with *E. coli* and examined at 4, 8, 12, 16, 20, and 24 h post infection. The CFU was 3.1×10^8 . The chemiluminescence method was used to quantify the level of MPO. The PMNs were divided into three groups: the control group, the HPI-infected group, and the Δ HPI-infected group. Data in the graphs represent the mean \pm SEM of at least 3 independent experiments. * $P < 0.05$; ** $P < 0.01$, analyzed by ANOVA.

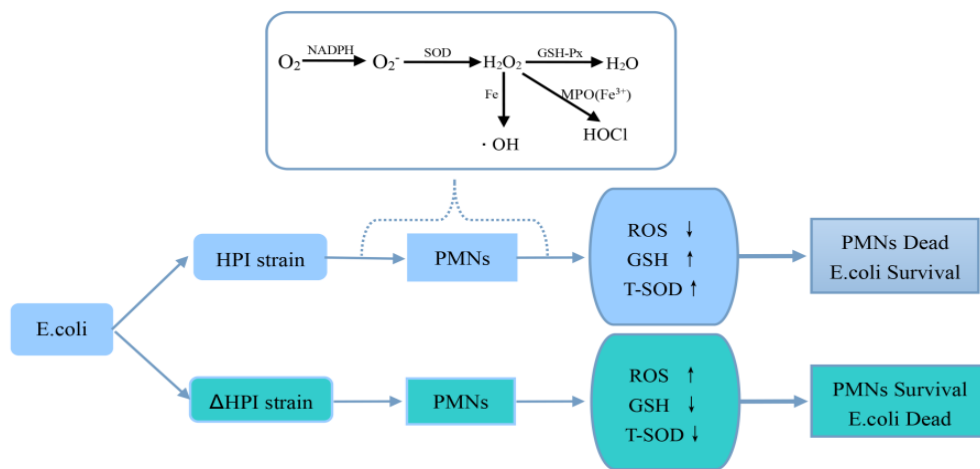


Figure 8: Schematic representation of the proposed mechanism of the respiratory burst in polymorphonuclear leukocytes (PMNs). When pathogens invade PMNs, nicotinamide adenine dinucleotide phosphate (NADPH) can catalyze oxygen into superoxide anion radicals (O_2^-), but O_2^- cannot cross the cell membrane. Furthermore, O_2^- can be catalyzed into hydrogen peroxide (H_2O_2) by superoxide dismutase (SOD). However, H_2O_2 has a low oxidative ability and thus cannot kill bacteria effectively. PMNs can catalyze other reactive oxygen species to kill bacteria. Fe^{3+} and myeloperoxidase (Fe^{3+}) catalyze H_2O_2 into HO and $HOCl$, respectively, which can effectively kill pathogens. In this reaction, H_2O_2 can be catalyzed into H_2O by antioxidant glutathione peroxidase (GSH-Px) in the case of self-injury caused by bactericidal reactive oxygen species (ROS). In this oxidant-antioxidant system, Δ HPI strains can induce a reduction in ROS and an increase in antioxidants (T-SOD, GSH-Px), but high-pathogenicity island (HPI) strains produce opposite effects. Consequently, when PMNs were infected with *E. coli*, the HPI strain effectively killed PMNs and survived in large numbers, while the outcome was reversed for the Δ HPI strain.

PMNs can kill invading pathogens by producing ROS. HPI-positive *E. coli* reduced the generation of ROS and increased the antioxidant levels, which eventually reduced the population of PMNs (Figure 8). PMNs infected with HPI knockout strains of *E. coli* yielded opposite results.

HPI are able to change the oxidative stress situation in PMNs, which might be useful for understanding the virulence of HPI-positive *E. coli*.

Funding

This study was supported by the National Natural Science Foundation of China (Grant No. 31260594 and 31660704), which supported study, collection and analysis. The Technology System Construction of the swine industry in modern agriculture in the Yunnan Province, which supported interpretation of data.

References

- El Kebir D, Filep JG (2013) Modulation of Neutrophil Apoptosis and the Resolution of Inflammation through beta2 Integrins. *Front Immunol* 4: 60.
- Ciz, M, Denev P, Kratchanova M, Vasicek O, Ambrozova G, et al. (2012) Flavonoids inhibit the respiratory burst of neutrophils in mammals. *Oxid Med Cell Longev* 6.
- Sakai J, Li J, Subramanian KK, Mondal S, Bajrami B, et al. (2012) Reactive oxygen species-induced actin glutathionylation controls actin dynamics in neutrophils. *Immunity* 37: 1037–1049.
- Ke Y, Chen Z, Yang R (2013) *Yersinia pestis*: mechanisms of entry into and resistance to the host cell. *Cell Infect Microbiol* 3: 106.
- Khajah M, Andonegui G, Chan R, Craig AW, Greer PA, et al. (2013) Fer kinase limits neutrophil chemotaxis toward end target chemoattractants. *J Immunol* 190: 2208–2216.
- Fukai T, Ushio-Fukai M (2011) Superoxide dismutases: role in redox signaling, vascular function, and diseases. *Antioxid Redox Signal* 15: 1583–1606.
- Lustgarten MS, Bhattacharya A, Muller FL, Jang YC, Shimizu T, et al. (2012) Complex I generated, mitochondrial matrix-directed superoxide is released from the mitochondria through voltage dependent anion channels. *Biochem Biophys Res Commun* 422: 515–521.
- Bréchar S, Plançon S, Tschirhart EJ (2013) New insights into the regulation of neutrophil NADPH oxidase activity in the phagosome: a focus on the role of lipid and Ca^{2+} signaling. *Antioxid. Redox Signal* 18: 661–676.
- Yu S, Long H, Lyu Q, Zhang Q, Yan Z, et al. (2014) Protective effect of quercetin on the development of preimplantation mouse embryos against hydrogen peroxide-induced oxidative injury. *PLoS One* 9: e89520.
- Hosakote YM, Komaravelli N, Mautemps N, Liu T, Garofalo, et al. (2012) Antioxidant mimetics modulate oxidative stress and cellular signaling in airway epithelial cells infected with respiratory syncytial virus. *Am J Physiol Lung Cell Mol Physiol* 303: L991-1000.
- Fernandez J, Wilson RA (2014) Characterizing roles for the glutathione reductase, thioredoxin reductase and thioredoxin peroxidase-encoding genes of *Magnaporthe oryzae* during rice blast disease. *PLoS One* 9.
- Sabater B, Martín M (2013) Hypothesis: increase of the ratio singlet oxygen plus superoxide radical to hydrogen peroxide changes stress defense response to programmed leaf death. *Front Plant Sci* 4: 479.
- Basheer Hasan D, Abdul Raman AA, Wan Daud WMA (2014) Kinetic modeling of a heterogeneous fenton oxidative treatment of petroleum refining wastewater. *Sci World J* 8.
- Suyama K, Watanabe M, Sakabe K, Otomo A, Okada Y, et al. (2014) GRP78 suppresses lipid peroxidation and promotes cellular antioxidant levels in glial cells following hydrogen peroxide exposure. *PLoS One* 9.
- Speth C, Brodde MF, Hagleitner M, Rambach G, van Aken H, et al. (2013) Neutrophils Turn Plasma Proteins into Weapons against HIV-1. *PLoS One* 8.
- Üllen A, Singewald E, Konya V, Fauler G, Reicher H, et al. (2013) Myeloperoxidase-Derived Oxidants Induce Blood-Brain Barrier Dysfunction In Vitro and In Vivo. *PLoS One* 8.
- Aiken ML, Painter RG, Zhou Y, Wang G (2012) Chloride transport in functionally active phagosomes isolated from Human neutrophils. *Free Radic Biol Med* 53: 2308–2317.
- Rakin A, Schneider L, Podladchikova O (2012) Hunger for iron: the alternative siderophore iron scavenging systems in highly virulent *Yersinia*. *Front Cell Infect Microbiol* 2: 151.
- Lv H, Henderson JP (2011) *Yersinia* high pathogenicity Island genes modify the *Escherichia coli* primary metabolome independently of siderophore production. *J Proteome Res* 10: 5547–5554.

20. Koczura R, Mokracka J, Kaznowski A (2012) The *Yersinia* high-pathogenicity island in *Escherichia coli* and *Klebsiella pneumoniae* isolated from polymicrobial infections. *Polish J Microbiol* 61: 71–73.
21. Zhang J, Wang X, Vikash V, Ye Q, Wu D, et al. (2016) ROS and ROS-Mediated Cellular Signaling. *Oxid. Med. Cell. Longev.*
22. Waldeck H, Wang X, Joyce E, Kao WJ (2012) Active leukocyte detachment and apoptosis/necrosis on PEG hydrogels and the implication in the host inflammatory response. *Biomaterials* 33: 29–37.
23. Zorov DB, Juhaszova M, Sollott SJ (2014) Mitochondrial Reactive Oxygen Species (ROS) and ROS-Induced ROS Release. *Physiol Rev* 94: 909–950.
24. Liu L, Zhang K, Sandoval H, Yamamoto S, Jaiswal M, et al. (2015) Glial lipid droplets and ROS induced by mitochondrial defects promote neurodegeneration. *Cell* 160: 177–190.
25. Adam M, Meyer S, Knors H, Klinke A, Radunski UK, et al. (2015) Levosimendan displays anti-inflammatory effects and decreases MPO bioavailability in patients with severe heart failure. *Sci Rep* 5: 9704.
26. Schieber M, Chandel NS (2014) ROS function in redox signaling and oxidative stress. *Curr Biol* 24: R453-R462.
27. Shaw PX, Stiles T, Douglas C, Ho D, Fan W, et al. (2016) Oxidative stress, innate immunity, and age-related macular degeneration. *AIMS Mol Sci* 3: 196–221.
28. Kordower JH, Olanow CW, Dodiya HB, Chu Y, Beach TG, et al. (2013) Disease duration and the integrity of the nigrostriatal system in Parkinson's disease. *Brain* 136: 2419–2431.
29. Landry WD, Cotter TG (2014) ROS signalling, NADPH oxidases and cancer. *Biochem. Soc Trans* 42: 934–938.
30. Ben Rejeb K, Benzarti M, Debez A, Bailly C, Savouré A, et al. (2015) NADPH oxidase-dependent H₂O₂ production is required for salt-induced antioxidant defense in *Arabidopsis thaliana*. *J Plant Physiol* 174: 5–15.
31. Lu X, Wang C, Liu B (2015) The role of Cu/Zn-SOD and Mn-SOD in the immune response to oxidative stress and pathogen challenge in the clam *Meretrix meretrix*. *Fish Shellfish Immunol.* 42: 58–65.
32. Li J, Wang LN, Xiao HL, Li X, Yang JJ (2014) Effect of electroacupuncture intervention on levels of SOD, GSH, GSH-Px, MDA, and apoptosis of dopaminergic neurons in substantia nigra in rats with Parkinson's disease. *Zhen Ci Yan Jiu* 39: 185–191.
33. Lloyd MM, Hadfield K, Grima M, Hawkins C (2014) Modulation of endothelial cell function by the myeloperoxidase-derived oxidant hypochlorous acid (HOCl) and its contribution to atherosclerosis. *Hypertension* 63: e170.
34. Ghoshal K, Das S, Aich K, Goswami S, Chowdhury S, et al. (2016) A novel sensor to estimate the prevalence of hypochlorous (HOCl) toxicity in individuals with type 2 diabetes and dyslipidemia. *Clin. Chim. Acta* 458: 144–153.

Author Affiliation

Top

Institute of Animal Science, Veterinary Practice, University of Hohenheim, Schwerzstr, 15/4, Stuttgart, Germany

Submit your next manuscript and get advantages of SciTechnol submissions

- ❖ 80 Journals
- ❖ 21 Day rapid review process
- ❖ 3000 Editorial team
- ❖ 5 Million readers
- ❖ More than 5000 
- ❖ Quality and quick review processing through Editorial Manager System

Submit your next manuscript at • www.scitechnol.com/submission